

**Self-assembly of a mixed-valence FeII-FeIII tetranuclear star**

Journal:	<i>Dalton Transactions</i>
Manuscript ID	DT-COM-03-2018-001241.R1
Article Type:	Communication
Date Submitted by the Author:	27-Apr-2018
Complete List of Authors:	Sertphon, Darunee; Walailak University, Functional Materials and Nanotechnology Center of Excellence Harding, Phimphaka; Walailak University, Chemistry Murray, Keith; Monash University, Chemistry Moubaraki, Boujemaa; Monash University, Chemistry Chilton, Nicholas; University of Manchester, Chemistry Hill, Stephen; National High Magnetic Field Laboratory, EMR Program Marbey, Jonathan; Florida State University, Department of Physics Adams, Harry; University of Sheffield, Department of Chemistry Davies, Casey; University of Otago, Department of Chemistry Jameson, Guy N. L.; The University of Melbourne, School of Chemistry Harding, David; Walailak University, Chemistry



Self-assembly of a mixed-valence Fe^{II}-Fe^{III} tetranuclear star

Darunee Sertphon,^{a,b} Pimphaka Harding,^a Keith S. Murray,^c Boujemaa Moubaraki,^c Nicholas F. Chilton,^d Stephen Hill,^{e,f} Jonathan Marbey,^{e,f} Harry Adams,^g Casey G. Davies,^h Guy N.L. Jameson^{h,i} and David J. Harding^{*a}

Received 00th January 20xx,
Accepted 00th January 20xx

DOI: 10.1039/x0xx00000x

www.rsc.org/

A unique self-assembled mixed-valence Fe^{II}-Fe^{III} tetranuclear star has been comprehensively characterised showing a large magnetic anisotropy at the peripheral Fe^{II} centres, ferromagnetic coupling between the iron centres and field-induced SMM behaviour.

The design and study of transition metal clusters with useful magnetic properties remains a considerable challenge. Single molecule magnets (SMMs) are of particular interest as they exhibit slow relaxation of magnetization with a barrier to spin reversal proportional to the uniaxial magnetic anisotropy and the squared spin of the cluster.^{1–8} The magnetic bistability of these clusters potentially permits their use in data storage applications and quantum computation.^{9–13} To be useful SMMs must be robust and retain their magnetic bistability when deposited on a surface.^{14,15} This is often not the case, for example [Mn₁₂O₁₂(O₂CR)₁₆(H₂O)₄] undergoes reduction upon deposition on Au(111) and loss of SMM behaviour.¹⁶

A series of particularly robust Fe^{II}₄ SMMs was first reported in 1999, and is based on the star shaped [Fe₄(dpm)₆(OMe)₆] (dpm = 2,2,6,6-tetramethyl-3,5-heptanedionate) molecule.¹⁷ Replacing the methoxides with two tripodal ligands, H₃L = R-C(CH₂OH)₃ gives [Fe₄(dpm)₆(L)₂] with improved SMM characteristics due to a change in symmetry from C₂ to D₃ resulting in an increase in the helical pitch of the Fe(O₂Fe)₃ core, thus increasing the magnetic anisotropy.^{18,19} The robustness of these Fe₄ stars has allowed them to be

deposited on gold,^{20–24} silicon²⁵ and boron nitride.²⁶ Unusually, their slow magnetic relaxation is retained on surfaces, which is the first step towards making the above applications a reality.

More recently, tridentate dianionic O,N,O ligands have been used notably the chiral *R* or *S*-2-[(*o*-Hydroxyphenyl)-methylideneamino]-2-phenylethanol ligands which impart their chirality on the cluster, [Fe₄(L')₆].^{27–29} Varying the substituents on the ligands allows tuning of the magnetic relaxation barrier (U_{eff}) from 0.5 – 11.0 K.²⁹ As with [Fe₄(dpm)₆(L)₂], subtle differences in the Fe coordination spheres are responsible for the differing magnetic properties.

Similar stars are formed using the O,N,O donor ligand *N*-methylmethylethanolamine (*N*-Me-dea). The star forms by self-assembly of [Fe(*N*-Me-dea)₂] around Fe^{III} to give [Fe{Fe(*N*-Me-dea)₂}₃] with U_{eff} = 14.2 K.^{30,31} In an analogous way, Takahashi *et al.*, in an attempt to make spin crossover hybrid materials, instead isolated [Fe{Fe(phsal)₂}₃] (phsal = *N*-(2-hydroxyphenyl)-salicylaldimine).³² Despite its structural similarity to the stars above, it is not a SMM.

In our continuing interest in tridentate N₂O donor ligands we selected 2-((1*H*-imidazol-2-yl)methyleneamino)phenol (2-H₂imap)³³ with the aim of preparing Fe^{III} spin crossover complexes. Unexpectedly, the primary product is a unique mixed-valence Fe^{II}-Fe^{III} star. Herein, we report the structure, magnetic and spectroscopic properties of [Fe₄(2-Himap)₆][NO₃]₃ **1**.

Complex **1** was synthesized by layering a MeOH solution of Fe(NO₃)₃·9H₂O on top of a warmed solution of the ligand, 2-H₂imap and NEt₃ (see ESI for details). After one week black crystals of the self-assembled cluster [Fe₄(2-Himap)₆][NO₃]₃ **1** are formed. Temperature and time are critical in isolating the cluster, as heating above 40 °C or harvesting the crystals too early gives the Fe^{III} monomer, [Fe(2-Himap)₂]NO₃·0.7MeOH **2** (Fig. S1–S2, S8 and Table S1). IR spectroscopic studies of **1** and **2** reveal imine and nitrate stretches in the expected positions, with ν_{C=N} being 18 cm⁻¹ lower in **2** than for **1**. A similar difference in the imine stretch is observed in the Co^{II}/Co^{III} redox pair [Co(2-Himap)₂]^{0/+}.³⁴ X-ray crystallography reveals that **1** is a star shaped cluster crystallizing in cubic Pa $\bar{3}$ (Fig. 1).

^a Functional Materials and Nanotechnology Centre of Excellence, Walailak University, Thasala, Nakhon Si Thammarat, 80160, Thailand

^b Now at: Department of Chemistry, Faculty of Science, Rangsit University, Phaholyothin Rd., Muang, Pathum Thani, 12000, Thailand

^c School of Chemistry, Monash University, Clayton, Victoria, 3800, Australia

^d School of Chemistry and Photon Science Institute, The University of Manchester, Oxford Road, Manchester M13 9PL, United Kingdom

^e Florida State University, Department of Physics, Tallahassee, FL 32306 USA

^f National High Magnetic Field Laboratory, 1800 E. Paul Dirac Drive, Tallahassee, FL 32310, USA

^g Department of Chemistry, University of Sheffield, Sheffield, S3 7HF, United Kingdom

^h Department of Chemistry & MacDiarmid Institute for Advanced Materials and Nanotechnology, University of Otago, PO Box 56, Dunedin, 9054, New Zealand

ⁱ School of Chemistry, Bio21 Molecular Science and Biotechnology Institute, 30 Flemington Road, The University of Melbourne, Parkville Victoria 3010, Australia
Electronic Supplementary Information (ESI) available: Experimental details, crystallographic details & figures, magnetic fits and CASSCF-SO calculations details, Mössbauer and EPR spectroscopic figures. See DOI: 10.1039/x0xx00000x

PXRD studies indicate that the single crystal structure is representative of the bulk material and ESI-MS studies in MeOH indicate that the cluster is stable in solution (see ESI, Figs. S4 and S5). The Fe1-O bond lengths are between 1.998–2.005(3) Å while the Fe2-N/O bond distances are much longer, 2.133–2.184(4) Å. This is consistent with the Fe1 and Fe2 centres being Fe^{III} and Fe^{II} respectively. This is, to the best of our knowledge, the first example of a mixed-valence Fe star cluster. The Fe1⋯Fe2 distance is 3.225 Å, while the Fe2⋯Fe2* distance is 5.586 Å and these are similar to the equivalent distances in other Fe^{III}₄ stars. Each molecule is chiral due to intramolecular π-π interactions between the 2-Himap ligands (Fig. S3), but as both enantiomers are present the structure overall is achiral.

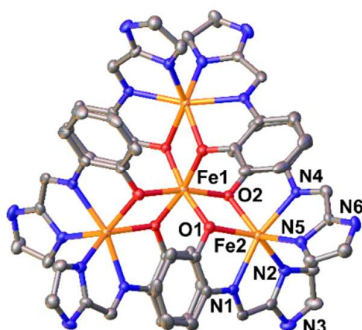


Figure 1 View of the star shaped cluster [Fe₄(2-Himap)₆][NO₃]₃. Hydrogen atoms are omitted for clarity.

Mössbauer spectra of **1** were recorded at multiple temperatures and show the presence of two subspectra above 20 K; a quadrupole doublet consistent with HS Fe^{II} and a singlet assigned to the HS Fe^{III} centre (Fig. S6 and Table S2). The ratio of the intensity of the two species is ~2:1, which is lower than the expected 3:1 ratio. We believe this is due to differing Lamb-Mössbauer factors of the Fe^{II} and Fe^{III} centres causing the relative intensities of the two species to not be equivalent, particularly at higher temperatures.³⁵

As the temperature is lowered the signals broaden, demonstrated by the temperature dependence of the full-width-at-half-maximum (FWHM) values for the transitions (Γ, Fig. S7d). Below ~15 K, the Fe^{III} signal undergoes intermediate relaxation and broadens, but does not completely collapse into the baseline. In contrast, the Fe^{II} signal remains visible as a distinct quadrupole doublet at all investigated temperatures; these changes mirror the magnetic transition (*vide infra*).

Magnetic measurements for **1** show $\chi_{\text{M}}T = 15.02 \text{ cm}^3 \text{ K mol}^{-1}$ at 300 K with $\chi_{\text{M}}T$ increasing slowly to a maximum of $28.43 \text{ cm}^3 \text{ K mol}^{-1}$ at *ca.* 8 K before decreasing rapidly (Fig. 2). The $\chi_{\text{M}}T$ value at 300 K is consistent with one non-interacting Fe^{III} and three non-interacting Fe^{II} centres, and the low temperature data shows evidence of a ferromagnetically coupled ground state. The minor temperature dependence of $\chi_{\text{M}}T$ above 150 K suggests that the intramolecular magnetic interactions are relatively weak; this, coupled with the presence of a possible orbital contribution to the magnetic moment of high-spin octahedral Fe^{II} centres make the

interpretation of the magnetic data fraught with difficulty. In order to get some insight into the local magnetic properties of the Fe^{II} sites to inform our interpretation, we have performed complete active space self-consistent field spin-orbit (CASSCF-SO) calculations (see ESI for details). These show that the Fe^{II} sites are well-described as $S = 2$, however are subject to a significant axial zero-field splitting (ZFS, $D \sim -17 \text{ cm}^{-1}$, $|E/D| \sim 0.12$), which arises from close-lying orbitally degenerate states. Interestingly, the main anisotropic axis for each of the Fe^{II} centres lies perpendicular to the plane of the Fe₄ cluster, and points towards the central Fe^{III} centre along a near-two-fold symmetry axis (Fig. S13). Given the significant ZFS of the Fe^{II} centres and possibly weak magnetic exchange, it is important to consider the non-collinearity of the local anisotropy axes. Therefore to model our data, we employ the following spin Hamiltonian in PHI³⁶:

$$\begin{aligned} \hat{H} = & -2J_1\hat{S}_1 \cdot (\hat{S}_2 + \hat{S}_3 + \hat{S}_4) - 2J_2(\hat{S}_2 \cdot \hat{S}_3 + \hat{S}_3 \cdot \hat{S}_4 + \hat{S}_4 \cdot \hat{S}_2) \\ & + D(\hat{S}_{z_2}^2 + \hat{S}_{z_3}^2 + \hat{S}_{z_4}^2) \\ & - 1/3(\hat{S}_2^2 + \hat{S}_3^2 + \hat{S}_4^2) \\ & + g\mu_B(\hat{S}_1 + \hat{S}_2 + \hat{S}_3 + \hat{S}_4) \cdot B \end{aligned}$$

Here, \hat{S}_1 is the spin operator for $S = 5/2$ of Fe^{III}, \hat{S}_{2-4} are the spin operators for $S = 2$ Fe^{II}, J_1 and J_2 represent the magnetic coupling between the central Fe^{III} and peripheral Fe^{II} centres (Fe1-Fe2), and the peripheral Fe atoms (Fe2-Fe2), respectively. g is the isotropic g -factor for the cluster, B is the applied magnetic field, and D is the single-ion axial ZFS of the Fe^{II} sites (we ignore E as CASSCF-SO predicts only a small rhombicity); we have rotated the local z -axis of each Fe^{II} site to point towards the central Fe^{III} ion, thus $\hat{S}_{z_{2-4}}$ are non-collinear. There are two possible solutions obtained when fitting the $\chi_{\text{M}}T$ and M vs. B data simultaneously: one with $D < 0$ (as suggested by CASSCF-SO) and one with $D > 0$. The former gives $J_1 = +2.77 \text{ cm}^{-1}$, $J_2 = -0.675 \text{ cm}^{-1}$, $g = 1.96$ and $D = -7.09 \text{ cm}^{-1}$ (Figs. 2 and S10-11); while the latter gives $J_1 = +2.62 \text{ cm}^{-1}$, and $J_2 = -0.738 \text{ cm}^{-1}$, $g = 2.03$ and $D = +14.0 \text{ cm}^{-1}$ (Figs. S9-11). Both solutions agree on the nature of the exchange interactions, where we see a weak ferromagnetic exchange between the Fe^{II} and Fe^{III} centres; antiferromagnetic coupling is observed in the related Fe^{III}₄ clusters. While the solution with $D > 0$ appears to model the high temperature $\chi_{\text{M}}T$ data better than the $D < 0$ solution, the low temperature magnetisation data (which is more sensitive to the details of the electronic structure) is better accounted for by the $D < 0$ solution; as $D < 0$ is also suggested by CASSCF-SO, we believe this to be the more likely description.

Given the ferromagnetic ground state and large anisotropy, we conducted *ac* susceptibility measurements to see if **1** showed slow magnetization relaxation and SMM behaviour. Plots of the out-of-phase susceptibilities, χ_{M}'' , as a function of *ac* frequency showed zero values in zero applied *dc* field; however frequency dependent “tails” were noted below 5 K in a static *dc* field of 3000 Oe; Fig. S12. This is in contrast with the $S = 5$ ground state [Fe^{III}₄(L)₂(dpm)₆] stars, L = alkoxide(3-),¹⁸ for which frequency dependent maxima in χ_{M}'' were observed in

zero dc field. Thus, our data indicate a lower U_{eff} barrier for **1** compared to the Fe^{III}_4 family of 3.5 – 17 K.

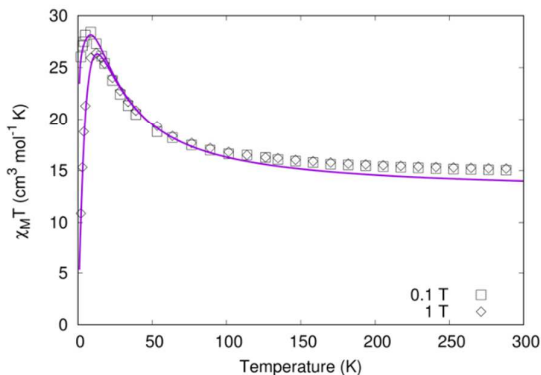


Figure 2 $\chi_M T$ vs. T plot of **1**. The purple lines represent the best fit ($D = -7.09 \text{ cm}^{-1}$) with the parameters given in the text.

Variable temperature, multi-high-field/frequency EPR measurements were performed on a constrained powder of **1**.³⁷ Fig. 3 shows a series of field-swept dI/dB spectra recorded at different frequencies in the range from 53 to 648 GHz, and a temperature of 5 K. Meanwhile, Fig. S14 plots the positions of the features in the spectra that disperse strongly with magnetic field. These can be divided into two groupings: the first set of resonances lie on a straight line that has a slope corresponding a g -value of 2.004 ± 0.004 , with zero offset (± 4 GHz) on the frequency axis; the second grouping of two broad resonances observed at the highest frequencies lie on straight lines that have identical zero-field intercepts of 344 ± 4 GHz, and slopes corresponding to g -values of 1.66 ± 0.05 and 2.61 ± 0.06 .

The $g = 2.004$ resonance consists of a sharp inflection superimposed on a broader shoulder. Such a signal suggests a weakly anisotropic species, most likely corresponding to $S = 5/2$ Fe^{III} with an isotropic d^5 electronic configuration.³⁸ Were such a signal to originate from the Fe^{III} constituent within the Fe_4 cluster, it would imply essentially no exchange coupling to the Fe^{II} centres. On the basis of the magnetic measurements, we feel that this scenario is highly unlikely. Consequently, we attribute the $g = 2.00$ signal to the Fe^{III} monomer **2** that is likely present in small quantities in the powder sample, which shows an isotropic magnetic moment (Fig. S8). It is difficult to compare the intensity of this signal with the broad high-frequency components because they are never observed within the same frequency/field window. However, one must recall that the dI/dB traces correspond to the 2^{nd} derivative of the actual spin susceptibility (proportional to the number of spins). Thus, isotropic $g = 2.00$ resonances are strongly amplified in the dI/dB traces relative to broad anisotropic ones (see below). Therefore, it is quite possible the level of contamination in the powder sample is below the 1% level, consistent with the PXRD studies (Fig. S5).

We also comment on a series of reproducible features observed close to zero-field (below 1 T) at the lower frequencies (< 320 GHz). The origin of these signals is not

presently clear. Similar signals have been observed in samples that undergo magnetic ordering and, hence, strong changes in magnetization at low fields. Again, this is not consistent with the magnetic properties of **1**, therefore likely signifying additional minor contamination of the powder sample.

The considerable zero-field splitting (ZFS) associated with the broad high-frequency signals is indicative of an appreciable magnetic anisotropy. Therefore, we associate these excitations with the coupled Fe_4 cluster **1**. Indeed, the coincidence of the zero-field offsets, and the temperature dependence of the two resonances suggest that they both originate from the ground state of the molecule. The reason there are two resonances is because the measurement was performed on a powder, i.e. they originate from different crystallite orientations within the powder, corresponding to turning points in the orientation dependence of the anisotropic EPR spectrum. As such, the unique zero-field intercept corresponds to the gap between the ground and first excited spin projection states of the cluster. Interestingly, simulations of the energy levels based on the $D < 0$ parameterization obtained from fits to the magnetic data suggest a ZFS of 300 GHz (10 cm^{-1}) from a set of six near-degenerate ground states to a set of six near degenerate excited states; this differs by only 13% from the value deduced by EPR measurements. Meanwhile, the $D > 0$ parameterization is completely inconsistent with the EPR results: simulations predict a ZFS of just 110 GHz (3.7 cm^{-1}) from the ground to first excited states. Therefore, the EPR measurements strongly favour the negative D parameterization. Indeed, given the relatively low information content of the magnetic data and the level of approximation inherent in the model, agreement to within 13% is very good.

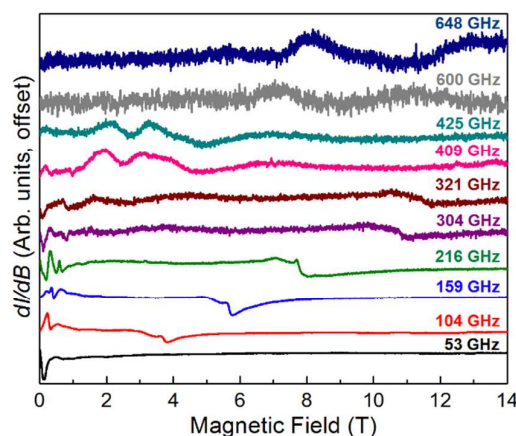


Figure 3 Normalized high-field EPR spectra on a constrained powder of **1**; the spectra were recorded in derivative mode, dI/dB (where I is the absorption intensity), using field modulation and lock-in detection. All measurements were performed at 5 K.

In conclusion we have prepared a unique mixed valence $\text{Fe}^{\text{II}}\text{-Fe}^{\text{III}}$ tetranuclear star by self-assembly. The star shows weak ferromagnetic coupling between the central and peripheral Fe centres. The star is a weak field-induced SMM with magnetic, EPR and CASSCF-SO studies all suggesting $D = -7.09 \text{ cm}^{-1}$ at the peripheral Fe^{II} centres. Preliminary studies

suggest that the outer Fe^{II} centres can be replaced with other metal ions and mixed metal stars of this type are now being pursued.

We thank the Thailand Research Fund (RSA5580028 and RSA5880048), the Australian Research Council (DP140101013) and the Ramsay Memorial Trust (fellowship to NFC) for funding this research. We also thank the Thailand Research Fund for financial support in the form of a Royal Golden Jubilee scholarship to DS (PHD/0135/2554). A portion of this work was performed at the National High Magnetic Field Laboratory (NHMFL), which is supported by the NSF (DMR-1157490) and the State of Florida. SH also acknowledges the support from the NSF (DMR-1610226).

Conflicts of interest

There are no conflicts to declare.

Notes and references

- G. Christou, D. Gatteschi, D. N. Hendrickson and R. Sessoli, *MRS Bull.*, 2000, 66–71.
- S. Dhers, H. L. C. Feltham and S. Brooker, *Coord. Chem. Rev.*, 2015, **296**, 24–44.
- T. Glaser, *Chem. Commun.*, 2011, **47**, 116–30.
- S. Goswami, A. K. Mondal and S. Konar, *Inorg. Chem. Front.*, 2015, **2**, 687–712.
- K. S. Pedersen, J. Bendix and R. Clérac, *Chem. Commun.*, 2014, **50**, 4396–415.
- H. Miyasaka, M. Julve, M. Yamashita and R. Clérac, *Inorg. Chem.*, 2009, **48**, 3420–3437.
- L. Rosado Piquer and E. C. Sañudo, *Dalton Trans.*, 2015, **44**, 8771–8780.
- D. N. Woodruff, R. E. P. Winpenny and R. A. Layfield, *Chem. Rev.*, 2013, **113**, 5110–5148.
- M. Affronte, *J. Mater. Chem.*, 2009, **19**, 1731.
- L. Bogani and W. Wernsdorfer, *Nat. Mater.*, 2008, **7**, 179–86.
- M. N. Leuenberger and D. Loss, *Nature*, 2001, **410**, 789–93.
- R. E. P. Winpenny, *Angew. Chem. Int. Ed.*, 2008, **47**, 7992–4.
- A. Ardavan, O. Rival, J. J. L. Morton, S. J. Blundell, A. M. Tyryshkin, G. A. Timco and R. E. P. Winpenny, *Phys. Rev. Lett.*, 2007, **98**, 57201.
- A. Cornia, M. Mannini, P. Sainctavit and R. Sessoli, *Chem. Soc. Rev.*, 2011, **40**, 3076.
- N. Domingo, E. Bellido and D. Ruiz-Molina, *Chem. Soc. Rev.*, 2012, **41**, 258–302.
- M. Mannini, P. Sainctavit, R. Sessoli, C. Cartier dit Moulin, F. Pineider, M.-A. Arrio, A. Cornia and D. Gatteschi, *Chem. - A Eur. J.*, 2008, **14**, 7530–7535.
- A. L. Barra, A. Caneschi, A. Cornia, F. De Fabrizi Biani, D. Gatteschi, C. Sangregorio, R. Sessoli and L. Sorace, *J. Am. Chem. Soc.*, 1999, **121**, 5302–5310.
- S. Accorsi, A.-L. Barra, A. Caneschi, G. Chastanet, A. Cornia, A. C. Fabretti, D. Gatteschi, C. Mortalo, E. Olivieri, F. Parenti, P. Rosa, R. Sessoli, L. Sorace, W. Wernsdorfer and L. Zobbi, *J. Am. Chem. Soc.*, 2006, **128**, 4742–55.
- A. Cornia, A. C. Fabretti, P. Garrisi, C. Mortalò, D. Bonacchi, D. Gatteschi, R. Sessoli, L. Sorace, W. Wernsdorfer and A.-L. Barra, *Angew. Chem. Int. Ed.*, 2004, **43**, 1136–9.
- M. Mannini, F. Pineider, P. Sainctavit, C. Danieli, E. Otero, C. Sciancalepore, A. M. Talarico, M.-A. Arrio, A. Cornia, D. Gatteschi and R. Sessoli, *Nat. Mater.*, 2009, **8**, 194–7.
- M. Mannini, F. Pineider, C. Danieli, F. Totti, L. Sorace, P. Sainctavit, M.-A. Arrio, E. Otero, L. Joly, J. C. Cezar, A. Cornia and R. Sessoli, *Nature*, 2010, **468**, 417–421.
- F. Pineider, M. Mannini, C. Danieli, L. Armelao, F. M. Piras, A. Magnani, A. Cornia and R. Sessoli, *J. Mater. Chem.*, 2010, **20**, 187–194.
- S. Ninova, V. Lanzilotto, L. Malavolti, L. Rigamonti, B. Cortigiani, M. Mannini, F. Totti and R. Sessoli, *J. Mater. Chem. C*, 2014, **2**, 9599–9608.
- M. J. Rodriguez-Douton, M. Mannini, L. Armelao, A.-L. Barra, E. Tancini, R. Sessoli and A. Cornia, *Chem. Commun.*, 2011, **47**, 1467–1469.
- G. G. Condorelli, A. Motta, G. Pellegrino, A. Cornia, L. Gorini, I. L. Fragalà, C. Sangregorio and L. Sorace, *Chem. Mater.*, 2008, **20**, 2405–2411.
- P. Erler, P. Schmitt, N. Barth, A. Irmeler, S. Bouvron, T. Huhn, U. Groth, F. Pauly, L. Gragnaniello and M. Fonin, *Nano Lett.*, 2015, **15**, 4546–4552.
- Y.-Y. Zhu, X. Guo, C. Cui, B.-W. Wang, Z.-M. Wang and S. Gao, *Chem. Commun.*, 2011, **47**, 8049–51.
- Y.-Y. Zhu, T.-T. Yin, S.-D. Jiang, A.-L. Barra, W. Wernsdorfer, P. Neugebauer, R. Marx, M. Dörfel, B.-W. Wang, Z.-Q. Wu, J. Van Slageren and S. Gao, *Chem. Commun.*, 2014, **50**, 15090–15093.
- Y.-Y. Zhu, C. Cui, K. Qian, J. Yin, B.-W. Wang, Z.-M. Wang and S. Gao, *Dalton Trans.*, 2014, **43**, 11897–907.
- R. W. Saalfrank, I. Bernt, M. M. Chowdhry, F. Hampel and G. B. M. Vaughan, *Chem. - A Eur. J.*, 2001, **7**, 2765–2769.
- R. W. Saalfrank, A. Scheurer, I. Bernt, F. W. Heinemann, A. V Postnikov, V. Schünemann, A. X. Trautwein, M. S. Alam, H. Rupp and P. Müller, *Dalton Trans.*, 2006, 2865–74.
- K. Takahashi, K. Kawamukai, T. Mochida, T. Sakurai, H. Ohta, T. Yamamoto, Y. Einaga, H. Mori, Y. Shimura, T. Sakakibara, T. Fujisawa, A. Yamaguchi and A. Sumiyama, *Chem. Lett.*, 2015, **44**, 840–842.
- J. Sanmartín-Matalobos, C. Portela-García, M. Fondo and A. M. García-Deibe, *Cryst. Growth Des.*, 2015, **15**, 4318–4323.
- D. Sertphon, K. S. Murray, W. Phonsri, J. Jover, E. Ruiz, S. G. Telfer, A. Alkaş, P. Harding and D. J. Harding, *Dalton Trans.*, 2018, **47**, 859–867.
- P. Gütllich, E. Bill and A. X. Trautwein, *Mössbauer Spectroscopy and Transition Metal Chemistry*, Springer-Verlag, Berlin/Heidelberg, 2011.
- N. F. Chilton, R. P. Anderson, L. D. Turner, A. Soncini and K. S. Murray, *J. Comput. Chem.*, 2013, **34**, 1164–1175.
- A. Hassan, L. Pardi, J. Krzystek, A. Sienkiewicz, P. Goy, M. Rohrer and L.-C. Brunel, *J. Magn. Reson.*, 2000, **142**, 300–312.
- R. J. Holmberg, T. Burns, S. M. Greer, L. Kobera, S. A. Stoian, I. Korobkov, S. Hill, D. L. Bryce, T. K. Woo and M. Murugesu, *Chem. - A Eur. J.*, 2016, **22**, 7711–7715.

TOC Entry**Self-assembly of a mixed-valence Fe^{II}-Fe^{III} tetranuclear star**

D. Sertphon, P. Harding, K. S. Murray, B. Moubaraki, N. F. Chilton, S. Hill, J. Marbey, H. Adams, C. G. Davis, G. N.L. Jameson and D. J. Harding

A self-assembled mixed-valence Fe^{II}-Fe^{III} tetranuclear star is reported that shows ferromagnetic coupling, field-induced single molecule magnetism and strong magnetic anisotropy at the peripheral Fe^{II} centres.

